Telescope Array Low Energy Extension (TALE)

Program Overview

Version 15

The TALE Collaboration

ABSTRACT:

This document is a general overview of the Telescope Array Low Energy Extension (TALE) project. We first describe the physics motivation behind the new observatory, then the ongoing analysis of the TA data, then the TALE detector elements and the status of their design and prototyping.

Table of Contents

1 Introduction

The Telescope Array (TA) experiment[1, 2] is an international collaboration involving research and educational institutions from Japan, U.S., China, Taiwan, and South Korea. For the U.S. part of TA, the main contributors are the University of Utah and University of Denver. Stage-1 of TA (see Section 3) is now nearing completion and will begin routine observations in 2008. This document will describe the concept and experimental design of the TA Low-energy Extension (TALE), which we are now proposing as a logical and cost-effective continuation of the TA program that offers many exciting possibilities.

The goal of the TA/TALE program is to study the sources of cosmic rays by measuring the characteristics (spectrum, composition, and anisotropy) of ultrahigh energy cosmic rays. The program aims to cover a wide energy range ($10^{16.5}$-$10^{20.5}$ eV), with a large aperture, good resolution, and good control of systematic uncertainties. The physics issues (what is the nature of the sources? and how do they accelerate particles to such high energies?) are among the most important questions in physics today, as identified by the Turner Panel[3].

2 TALE Physics

Finding the sources of Ultra High Energy Cosmic Rays (UHECRs) has proven to be an elusive goal. The most direct approach, the search for arrival direction anisotropy, has thus far yielded no conclusive results. Alternately, there is a great deal of information available in the form of structures in the energy spectrum of cosmic rays and in the measures of their composition. From low energy to high, these include (a) the knee of the spectrum occurs at about $\sim 3\times10^{15}$ eV, (b) the second knee in the middle of the 10^{17} eV decade, (c) the ankle at $\sim 4\times10^{18}$ eV, and (d) the Greisen-Zatsepin-K'uzmin (GZK) cutoff[4, 5] from photo-pion production in the Cosmic Microwave Background Radiation (CMBR) at $\sim 6\times10^{19}$ eV. Judging from the evolution of the mean depth of shower maximum, $\langle X_{max} \rangle$, the crossover from galactic to extra-galactic cosmic ray flux starts below, and appears complete by about 1×10^{18} eV, while some other, more model-dependent measures give a higher transition energy. Thus, in addition to continuing the search for anisotropy, a primary focus of UHECR experiments should be to gather information needed for the accurate interpretation of these features, in order to shed light on the basic questions.

Two workshops have been held in Aspen, Colorado to discuss the structures observed in the cosmic ray data and their interpretation: (a) the "Workshop on Physics at the End of the Galactic Cosmic Ray Spectrum" in April, 2005, and (b) the "Aspen Workshop on Cosmic Ray Physics" in April, 2007. These workshops were jointly sponsored by Rutgers University, the University of Utah, and the U.S. National Science Foundation. They were followed by a great deal of discussion on the same issues at the International Cosmic Ray Conference in Merida, Mexico, in July, 2007.

These meetings identified several topics of great interest. Of relevance here is the spectral region from above the first knee ($\sim 3\times10^{15}$ eV) to the GZK cutoff ($\sim 6\times10^{19}$ eV). From the low energy side, it has become clear that while supernova acceleration is still a leading contender for explaining the cosmic ray flux below the first knee, the galactic spectrum above this spectral break is poorly understood. Similarly, little is known about the endpoint of the galactic cosmic ray spectrum (putatively the second knee). A full explanation for the observed spectrum in the transition region may well require a new galactic source.

At the same time, more detailed studies of the propagation of extra-galactic cosmic rays indicate that the e^+e^- energy loss mechanism (also from CMBR interaction) will excavate a dip structure just below the GZK pileup. There are in fact suggestions that this dip structure, which seems to correspond to the ankle at ~4×10^{18} eV, may be a much more robust signature of interaction with the 2.7°K black body radiation than the GZK cutoff itself. This is discussed, for example, by Berezinsky *et al*. in reference [6]. For a discussion of the effects of the composition, on the spectrum in the ankle region see Allard *et al*. in [7]. Taking both the HiRes spectrum [8] and mean $X_{\max}$ [9] results into consideration simultaneously, the results of Allard *et al*. [7] could be interpreted to support the e^+e^- production interpretation of the ankle[10].

It seems clear that the galactic flux will be heavier than the extra-galactic one. This coupled with the fact that the ankle/dip structure occurs just above the second knee indicate that the key for disentangling the galactic termination from the extra-galactic flux lies in the measurement of cosmic ray composition. Hence, the workshops concluded that new experiments with the capability of measuring the flux and composition from just above the "first" knee to the GZK cutoff are considered of high priority. Of particular importance is the seamless inter-calibration of the different experimental techniques at one site. Our proposal builds on these recommendations from the workshops and community consensus.

2.1 Interpretation of HiRes Results

Two of the most important findings of the HiRes experiment are shown in Figure 1. The left half of Figure 1 shows the spectrum of cosmic rays as measured by the HiRes-I and HiRes-II detectors observing in monocular mode[8]. The features known as the "ankle", at the energy of $10^{18.65}$eV, and the GZK suppression, above $10^{19.75}$ eV, are clearly evident. In a recent publication[11] the HiRes collaboration announced the observation of the GZK cutoff with statistical significance of about five standard deviations. Above the GZK threshold of $10^{19.75}$ eV, the spectrum falls very steeply, with a power law fit of $E^{-5.1}$. References [8, 11, 12] include detailed discussions of systematic uncertainties in this flux measurement along with numerous citations to supporting publications.

The right half of Figure 1 shows a plot of the mean value of the depth of shower maximum, $\langle X_{\max}\rangle$, vs. log(E), as measured by the HiRes Prototype – MIA hybrid detector[13] and by the HiRes stereo detector [9, 14]. The slope of the fit, or *elongation rate*, is 93 g/cm^2/decade below ~10^{18} eV. However, the elongation rate decreases dramatically to 55 g/cm^2/decade at higher energies. In addition, the width of the X_{max} distribution is narrow at the lower energies, and becomes wider through ~10^{18} eV, indicative of a light composition. The broadened X_{max} distribution is then maintained to the highest energies measured. These observations lead naturally to the interpretation of a changing composition (becoming lighter) up to ~10^{18} eV, and remaining light above this energy. These results support a picture of a heavy galactic cosmic ray flux giving way to an extra-galactic cosmic ray flux of light composition near ~10^{18} eV. In this picture, the two spectral features above 10^{18} eV would thus be caused by interactions of extra-galactic protons with CMBR photons: the excavation of the ankle/dip by e^+e^- pair production[6, 7, 10], and the suppression of UHECR flux via photo-pion production above the GZK cutoff.

While this interpretation of the cosmic ray structure and composition is encouraging, the data and the experiments on which it is based were systematically limited by their small dynamic range in energy. The inference of an "early" (below ~10^{18} eV) transition from heavy to light

composition depends on the combined data from a hybrid experiment (HiRes/MIA), and the HiRes stereo experiment, which overlap by only ~1/4 of a decade in energy.

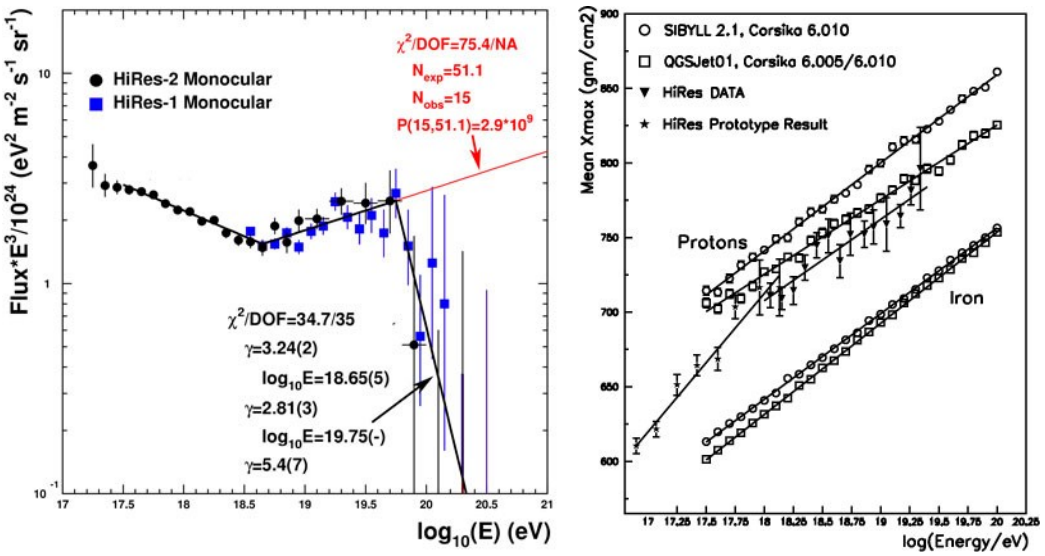

Figure 1: Left: The HiRes Monocular Spectrum showing the GZK cutoff [4, 5]. Right: Mean depth of shower maximum X_{max} vs. energy, measured by the HiRes/MIA and HiRes stereo experiments.

An alternative interpretation of the spectrum shown in Figure 1 is that the ankle forms the galactic/extra-galactic transition (with galactic sources giving the lower energy and extra-galactic the higher energy parts of the ankle). Here one should see a heavy composition giving way to a light one at about $10^{18.6}$ eV. Therefore the interpretation of the ankle either as e^+e^- energy loss, or as the galactic/extra-galactic transition, is critically dependent on composition measurements. At ICRC 2007, V. Berezinsky emphasized that the most important measurements to be made in UHE cosmic ray physics are on composition in the 10^{17} eV decade[15], because they represent the only means by which the interpretation of the ankle (e^+e^- production or galactic/extra-galactic transition) can be clarified.

The third feature of the ultrahigh energy spectrum, called the "second knee", has been seen by several previous experiments, however it is just too low in energy for the HiRes experiment to observe it convincingly. Moreover, while it has been observed by several experiments, none has a convincing energy scale. The second knee can be seen clearly when one normalizes each of the experiments, but in this process all information about the true energy of the feature is lost.

It is vital that the full energy region from below the second knee to the GZK cutoff should be surveyed by a single, seamless set of measurements with well understood resolution and systematics. This is exactly what TA and TALE will achieve.

2.2 Spectrum and Composition Studies with TALE

The possibility of post-GZK flux as a signpost to new physics has dominated discussion in the UHE cosmic ray community over the past ~15 years. The collective interest of the field has resulted in the construction of several experiments specializing in this energy region. However, this question is now settled. The HiRes experiment has observed the GZK cutoff[11] , and the Pierre Auger experiment has confirmed the appearance of the cutoff [16]. The observation of the GZK cutoff tells us several important things: first, the maximum energy of extra-galactic sources

is higher than the GZK energy; second, at the highest energies cosmic rays are at least 90% protons: if the proton fraction were smaller, the flux shown in Figure 1 above the GZK cutoff would be higher.

While finding specific sources of cosmic rays is clearly important, determining the maximum energy, spectral index, and evolution parameter of the sources is equally significant. The details of the spectral shape, measured with sufficient precision, have the potential of giving us this information. The ankle is a very important feature of the spectrum. It also provides a calibration point for the energy scales of experiments, as was emphasized by V. Berezinsky at ICRC 2007[15].

Performing fits to the combination of spectrum and composition allows one to construct a model of cosmic ray sources that is surprisingly detailed. As an example, we fit the HiRes spectrum shown in Figure 1 to a model where the heavy component is assumed to be galactic in origin, and the light component extra-galactic[17]. In this model all extra-galactic sources are given the same power law spectral index γ, maximum energy $E_{max}=10^{21}$ eV, and an isotropic distribution modified by a factor $(1+z)^m$, where z is the redshift and m is called the evolution parameter; this exponent takes into account the recent evolution of the sources and the Universal Expansion. The fitting procedure includes energy losses in interactions with extra-galactic protons and the CMBR, as well as the Hubble expansion. The fit parameters are the normalization, γ, and m.

In Figure 2 we see the results of these fits first for varying spectral indices and next for varying evolution parameters. The fits show that the region of the ankle is sensitive to the value of γ, and that the region just below the ankle is sensitive to the value of m. Therefore, these key source parameters can be measured independently. This spectral sensitivity to cosmological features reinforces the importance of the ankle of the cosmic ray spectrum, and of measurements in this energy range.

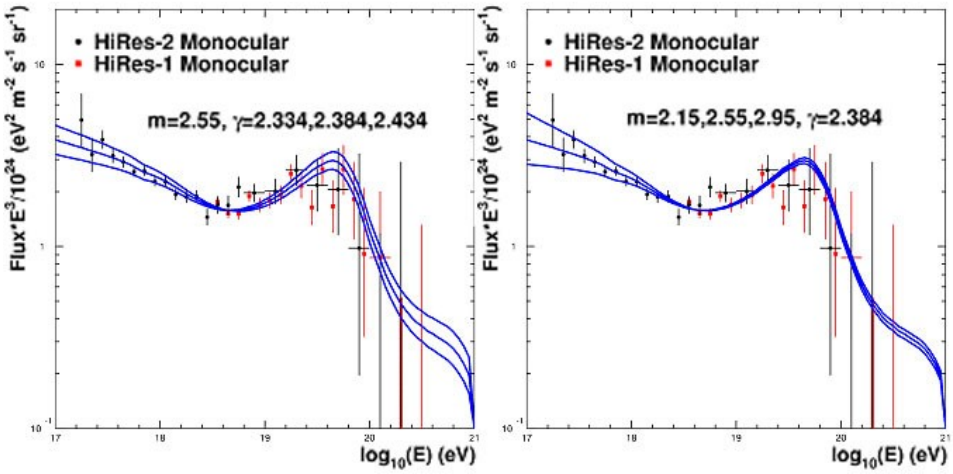

Figure 2: Effect of changing the spectral index, γ, and evolution parameter, m, in fits to the HiRes spectrum, showing that the ankle region is sensitive to γ, and that the region just below the ankle is most sensitive to m.

Figure 3(a) shows a decomposition of the extra-galactic spectrum from our energy-loss model for sources grouped in shells of redshift, z. This plot shows clearly how the GZK cutoff develops as well as how the ankle and pileup in the second knee region occur. In particular, it

illustrates the *fractionation* of extra-galactic events in energy by redshift. For example, the total cosmic ray flux at $10^{17.8}$ eV is dominated primarily by the shell of sources near z=1, and the contribution of the shell at z=0.1 to this energy range is lower by an order of magnitude. While this correlation between energy and redshift is not exactly one-to-one, it is quite significant.

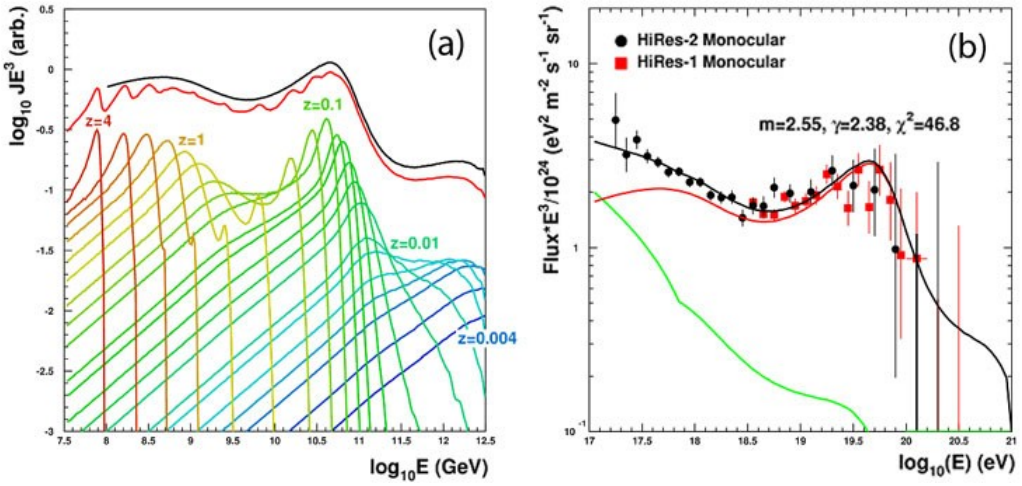

Figure 3: (a) Contributions from sources in shells in redshift to our energy loss model. (b) The HiRes monocular spectrum fitted to a model including extra-galactic sources (red), galactic sources (green); the sum of the two components is shown in black.

Based on this *E*-*z* correlation, the energy spectrum can thus be used to determine the evolution of extra-galactic sources of cosmic rays. In fits to extra-galactic sources, the evolution parameter, *m*, is introduced to take into account the evolution of relatively nearby sources. The result of this fit to the HiRes spectrum is given in Figure 3(b). To go further, using the energy/redshift correlation, one could fit the data to a model with a more complicated evolution in redshift. However, the current state of the world's data is not good enough for this: simultaneous measurements of spectrum and mean X_{max} do not cover a wide enough range in energy with well understood resolution and systematics. The HiRes data, for example, does not extend low enough to cover the second knee. In addition, it is significant to note that this simple two-component model fit to HiRes data in Figure 3(b) does not predict a second knee at all.

The *second knee* has been observed by four previous experiments[13, 18-22]. As seen in Figure 4, the energy scales of these detectors differed by about a factor of two, so the energy at which this spectral break occurs is quite uncertain. However, each data set shows a definite softening (break) in the power law spectral index (that we call the *second knee*). When the energy scales are adjusted in the right half of Figure 4, the four spectra can be made to align simultaneously in normalization (flux) and in the location of the break. Thus, while we know the break in the spectrum exists, its energy is uncertain, except that it occurs somewhere in the mid-10^{17} eV decade. No real progress on understanding this important feature can occur until one single experiment measures all three spectral features of the UHE cosmic ray regime.

In order to understand the second knee, one will need to fit the spectrum near it to power laws, and to an energy-loss model. This is a process that will require a good lever arm below as well as above the break. From our experience in fitting the HiRes spectrum[17], we know that one must push the minimum energy to at least $10^{16.5}$ (not $10^{17.0}$) eV. Similarly, at the high end of the

spectrum, one needs good sensitivity over the GZK cutoff region that is at least comparable to HiRes. The proposed TA/TALE experiment is uniquely positioned to accomplish all these goals.

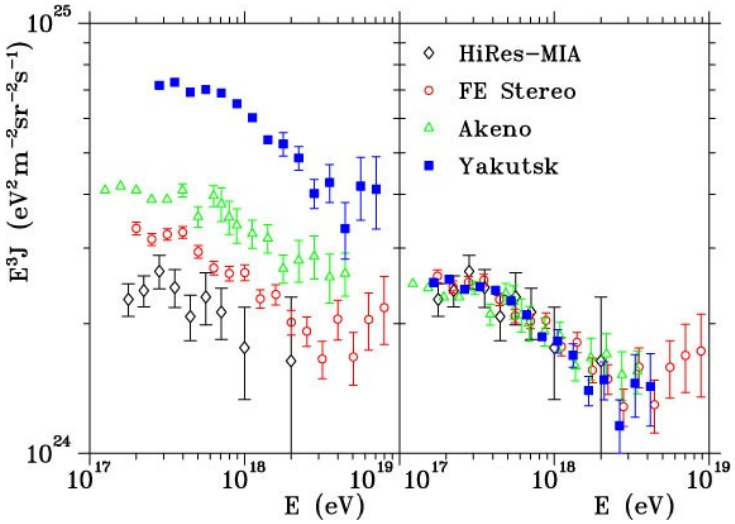

Figure 4: Left: Cosmic ray spectra measured by the Fly's Eye[18, 19], HiRes/MIA[13, 20], Akeno[21], and Yakutsk[22] experiments. Each shows a flat part, a break, and a falling part (on an E^3J plot, where J denotes the differential flux). Right: Aligning the flat parts of the spectra from the four experiments, the spectral feature known as the second knee appears at the same energy, about $10^{17.5}$ eV. Below this energy the spectrum is flat (on an E^3J plot).

Composition measurements in the $10^{16.5}$ -$10^{18.5}$ eV range, from X_{max} distributions and from the μ/e ratio of showers, will be very important. With reliable and redundant measurements of the composition, one can also selectively analyze the heavy or light parts of the event sample to see where the second knee presents itself. The TALE tower detector is necessary for this measurement. The second knee's presence in the heavy part of the data would indicate that the second knee is a galactic effect. Conversely, a second knee with light composition would suggest an extra-galactic origin for the effect.

The question of the origin of the ankle is not yet settled, although the preponderance of the evidence may indicate that it is excavated by e^+e^- pair production in collisions between cosmic ray protons and photons of the CMBR. A survey of the various models of the cause of the ankle was performed by V. Berezinsky in his invited talk at the 2007 ICRC [15]. Figure 5 shows a figure from his publication illustrating the two main models. The left panel shows a model where there is an "early" galactic-extragalactic transition at 10^{18} eV, and the ankle is excavated by e^+e^- pair production interactions between cosmic ray protons and photons of the CMBR. The right panel shows a model where the galactic cosmic rays, of heavy composition (Fe), dies away an order of magnitude higher in energy, letting the extragalactic component then show through. The ankle is at the midpoint of this transition.

The TA/TALE system of detectors is designed to distinguish between these two models. Figure 6 shows what the result of three years of TA/TALE data collection would be, in these two scenarios. Two comments can be usefully made about this figure. First we will be able to resolve the difference between the models in a very clear fashion. Second, it is necessary to have the ENTIRE suite of detectors of TA/TALE to perform a clear resolution of this important question.

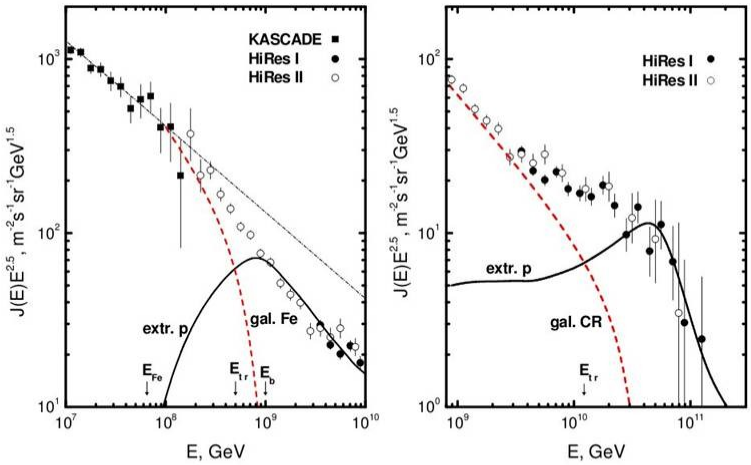

Figure 5. Two models of the cause of the ankle structure in the cosmic ray spectrum. The left panel shows an "early" termination of the galactic spectrum of cosmic rays, where the composition would be heavy (Fe) up to 10^{18} eV, and the ankle is caused by e^+e^- pair production. The right panel shows a model where the galactic component of the cosmic rays dies off, and the extragalactic component picks up, with a transition at 10^{19} eV, with the ankle appearing due to the sum of the two.

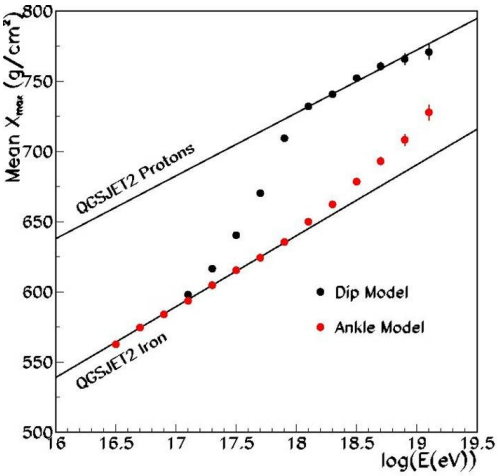

Figure 6. Composition Results of the TA/TALE experiment after three years of running, in two scenarios regarding the cause of the ankle of the cosmic ray spectrum. The black data points would be the result if there were an "early" galactic-extragalactic transition at 10^{18} eV and e^+e^- pair production excavated the ankle. The red data points would be the result if the ankle were caused by the galactic-extragalactic transition itself.

The details of the TALE experimental design are provided in Section 4. In interpreting spectrum and composition data together, each energy range gives us an important piece of information about the sources. A summary of the astrophysics specific to the different part of the TA/TALE energy range is given in Table 1.

Table 2 summarizes the statistical power of HiRes and TA/TALE data collected over a five year period, and estimates the accuracy achievable in the measurement of the extra-galactic power law (γ) and evolution parameter (m).

Energy Range	What we learn about extra-galactic sources
$10^{19.8}$ eV and up	Pion production from CMBR
$10^{18.0}$ to $10^{19.4}$ eV	Mean spectral index at the source
$10^{18.0}$ to $10^{18.7}$ eV	Evolution parameter
$10^{18.0}$ to $10^{19.4}$ eV	Pair production from CMBR
$10^{16.5}$ to $10^{18.7}$ eV	galactic/extra-galactic transition
$10^{16.5}$ to $10^{18.0}$ eV	The cause of the second knee.

Table 1: A summary of what we can learn from cosmic rays in different energy ranges within the coverage of the TA/TALE Experiment.

Experiment	$>10^{19}$eV	$10^{18\text{-}19}$eV	$<10^{18}$eV	γ	m	Structures Seen
HiRes Stereo	400	1500				GZK
HiRes Mono	500	6000	1000	$\pm$0.05	$\pm$0.03	Ankle + GZK
TA SD	1500	15000				GZK
TA Stereo	300	6000				Ankle + GZK
Tower			50000			Second Knee
TA/TALE total	1750	20000	50000	$\pm$0.02	$\pm$0.01	Second Knee, Ankle, GZK

Table 2: A comparison of the number of events expected from HiRes and TA/TALE for five years of observations and the corresponding physics potential.

2.3 Anisotropy Studies with TALE

Anisotropy studies with cosmic rays are difficult as a means of directly identifying the sources of cosmic rays due to the bending of charged nuclei by magnetic fields. Nevertheless, the observation of significant anisotropy would have such important consequences. Therefore, the field continues to emphasize this method. At this point, there are only four hints of anisotropy in the available UHECR data:

1. The direction of the AGASA triplet[23-25] and the HiRes event contained therein may represent a point source[26]. While it is currently of low statistical significance (~0.005)[26], this interpretation will be tested by TA data. The triplet is in Ursa Major and cannot be seen from Argentina.

2. HiRes has observed a correlation at the threshold of statistical significance between stereo events and BL-Lac objects [9]. These are a class of blazars with their jet aligned toward the

Earth, and are extra-galactic objects. The correlation is surprising since the apparent association is consistent with the 0.6 degree resolution of HiRes stereo data. If, however, these events are protons as the HiRes composition and spectral data would suggest, their trajectories should be deflected by the galactic magnetic field by more than a degree. Heavier nuclei would suffer even greater bending. For the correlation to be real, either the primaries involved must be neutral, or they are entering the Galaxy in locations where the galactic magnetic field is weak. This signal will be confirmed or rejected by TA data.

The Pierre Auger experiment has searched for correlations with BL Lac sources and has not found any[27]. However, very few of the sources found to correlate in the northern hemisphere can be seen from Argentina, and different telescopes (using different selection techniques) have identified the BL Lac samples in the two hemispheres. Therefore, at this time it is not clear if the Auger upper limit is relevant to the HiRes BL Lac correlations.

The TA experiment will have the highest sensitivity for high-resolution anisotropy studies of any experiment. A quantitative measure of this sensitivity is the time-averaged aperture of the experiment divided by the square of the resolution. Table 3 lists the aperture, resolution, and the point source sensitivity for HiRes stereo, TA stereo, the TA ground array, the Auger surface detector, and TA hybrid stereo, all at 10^{19} eV. With this energy threshold the BL Lac correlation is maximized in the current data sets. We note that TA hybrid-stereo events have a greater sensitivity to point sources than all other experiments by a significant factor.

Experiment	***Aperture (km^2sr)***	***Resolution (deg)***	***Point Source Sensitivity (Area/resolution^2)***
HiRes Stereo	300	0.5	1200
TA Stereo	185	0.5	740
TA Ground Array	1500	1.5	667
Auger SD	6600	1.5	2933
TA hybrid stereo	110	0.1	11000

Table 3: A comparison of the time-averaged aperture, angular resolution, and point-source sensitivity of recent UHECR experiments with that of TA operating in different analysis modes.

3. The AGASA experiment saw a deficit of events near, but not exactly at, the galactic anti-center[28]. There seems to be a deficit there also in the HiRes-II data[29]; the chance probability is calculated to be 0.0014, which corresponds to about 3.2 standard deviations significance. This is not a high enough significance to constitute an observation, so this must be tested and confirmed or rejected by future TA data. The galactic anti-center is very difficult for the Pierre Auger experiment to see since it is at about 70 degrees zenith angle from their site.

4. The Auger Collaboration has recently published [30] their finding of a correlation between high energy events and AGN's from the Veron-Cetty catalog[31]. They divided their data into two parts. For the first half, they scanned for the parameters which maximized the sensitivity of their search (the minimum energy, E_{min}, the maximum redshift, z_{max}, and the largest correlation

angle, θ_{max}). Their choice was (E_{min}, z_{max}, θ_{max}) = ($10^{19.75}$ eV, 0.018, and 3.1°). They found 15 events above E_{min} in the first half of their data. They then applied these cuts to the second half of their data and found 8 correlated events out of 13 total, where they expected about 3 random correlations. They quote the chance probability for the second part result as being 0.0017, which corresponds to about 3 standard deviations. This is not of high statistical significance. In the paper, the Auger collaboration comments that these parameters form a consistent picture of this anisotropy signal: (1) high energy events experience the least bending by intervening magnetic fields (2) This high energy (at and above the GZK cutoff) means that the source should be quite close, hence a relatively nearby z_{max} and (3) Above E_{min}=$10^{19.75}$ eV, 2°-4° of bending should be expected from the galactic magnetic field alone.

If the Auger result is valid, a correlation with AGN's in the southern hemisphere should exist in the northern hemisphere as well. Therefore, we examined the HiRes stereo data to test this hypothesis [32]. Judging by the normalization of their spectrum, at about 1 EeV the Auger energy scale is about 20% lower than that of HiRes, but at 56 EeV it seems to be within about 10%. For this correlation analysis we have lowered the energy scale of the HiRes stereo events by 10% to make it similar to the high energy part of the Auger experiment. Using the Auger selection criteria, we found 2 correlated events out of 13 where we expected 3 randomly. Thus, the HiRes data does not support the Auger contention. However, these experiments are working in the very-small-statistics regime. These results must be tested using further Auger data in the southern hemisphere and TA data in the north.

With considerably less obscuration of the Galaxy than Auger has, the TA experiment will be in an excellent position to pursue a follow-up study. In any case, a very important aspect of the TA experiment will be to test these hints of anisotropy with improved sensitivity and to search for others.

2.4 Correlations with Local Large Scale Structure

An example of the difficulty of searching for anisotropy in UHECR pointing directions is given by the HiRes search for correlations between their high energy events' pointing directions and local large scale structure (LSS) [33]. Here we are assuming that the sources of UHECR's are correlated with galaxies' locations on the sky. We made a model of the local large scale structure using the 2 Micron Redshift Survey, the most complete survey of galaxies located within 250 Mpc of us. By weighting the galaxies of the survey we transformed the flux-limited survey to a volume-limited density map of galaxies on the sky, and weighted each galaxy by $1/r^2$ and the exposure of the HiRes stereo data. If there were no magnetic fields between the sources and us one would expect that the pointing directions of the data would follow this density map. Since the galactic and extragalactic magnetic fields are known poorly we chose to represent their effect by an overall bending angle, which we used as an input parameter. We then compared the distribution of the data to the weighted density map modified by the magnetic bending angles using the Kalmogorov-Smirnov (K-S) test, using bending angles between 1° and 15°. We also performed the same test using an isotropic model. We chose three *a priori* minimum energies, where the searches described above found hints of anisotropy: 10, 40, and 57 EeV. About 40% of events at 10 EeV originate within a 250 Mpc sphere, and for 40 EeV (57 EeV) about 70% (100%) originate within 250 Mpc of us. From this one would expect to see lower correlation with LSS at 10 EeV than at the higher energies.

The results (K-S probabilities) are shown in Figure 7. Here the K-S probability is plotted against the magnetic bending angle, for the three minimum energies. The shaded area is where the data disagrees with the model at the 95% confidence level. The isotropic model is shown in the upper panel, and agreement is found between the model and data for all three energy cuts. As expected, for the 10 EeV energy cut not much can be said. But for 40 and 57 EeV the LSS model disagrees with the data at the 95% confidence level for magnetic smearing angles up to 10°. This is a surprising result, since magnetic bending is expected to be considerably less than this. It may indicate that galactic and/or extragalactic magnetic fields are larger than expected. This result needs to be confirmed by a future experiment in the northern hemisphere with larger statistics. The TA/TALE experiment will equal the statistics of HiRes stereo in early 2010, then go on to collect higher statistics.

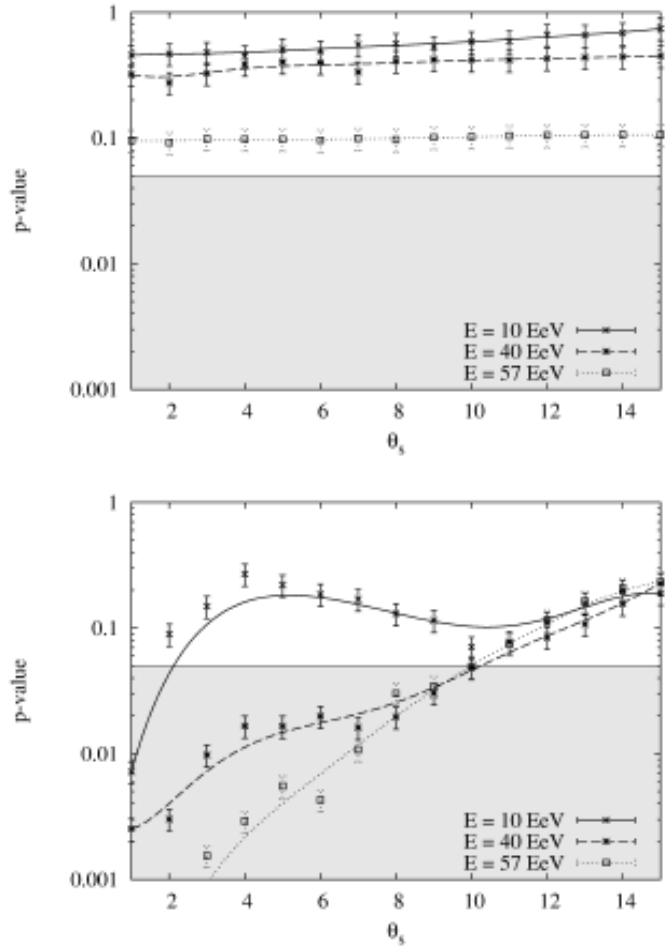

Figure 7. Tests of the hypothesis that HiRes stereo events' pointing directions are correlated with local large scale structure (LSS) of the universe (within 250 Mpc). Kolmogorov-Smirnov probability values are plotted against the magnetic smearing angle, θ_s, due to galactic and extragalactic magnetic fields. Three minimum energy cuts are shown: 10, 40, and 57 EeV. In case of disagreement of data and the models we choose *a priori* to quote 95% confidence levels (shown as shaded areas in the graphs). The upper panel, of an isotropic model, shows agreement with the data for all energies; the lower panel, of the LSS model, shows disagreement between the data and the model for smearing angles up to 10°.

3 TA Main Surface Array and Fluorescence Stations

The Telescope Array is a hybrid ultra-high energy cosmic ray (UHECR) observatory located in west-central Utah. The original TA experiment consists of a ground array of 507 scintillation counters placed in a square grid of 1.2 km spacing. The location and layout of TA experiment is shown in Figure 8. Three fluorescence detector (FD) stations, shown as red squares in Figure 8, overlook the ground array. The fluorescence stations are designated TA-FD0, TA-FD1, and TA-FD2, located at Black Rock Mesa (BRM: southeast corner), Long Ridge (LR: southwest corner), and Middle Drum (MD: north corner), respectively. The red cross shown at the center of the array represents the location of the Central Laser Facility (CLF) that houses a steerable UV laser at the middle of the field of view of all three FD stations. The positions of the surface detector (SD) counters are marked by blue diamond symbols.

Each SD counter consists of two layers of 1.0cm thick plastic scintillator, 3.0 m^2 in area. Light from energy deposition is collected using wavelength-shifting optical fibers that are embedded in extruded grooves in the surface of the plastic. The two ends of the fibers from each layer are glued together and coupled to PMTs. The use of the fibers gives good readout uniformity, and the twin layers provides redundant coincidence signals from charged particles. The analog signal from each PMT is digitized by a 50MHz, 12-bit Flash analog-to-digital converter (FADC). Each counter is also equipped with a GPS clock and a communication system. The entire counter is powered by a single 240W solar panel with deep cycle batteries. To minimize the impact on plant and animal life, the counters sit on an elevated frame and the completed detectors were lifted into place by helicopters.

The scintillator detectors are set to trigger at a signal equivalent to 1/3 minimum ionizing particle (MIP). Coincident triggers (within 8 μs) from ≥3 adjacent counters, and with a minimum of 3 MIPs each, constitute an event trigger, initiating readout of the ground array. Three communications towers, located near the FD stations, are used to form coincidence triggers and to relay control signals and data between the central facility at BRM and the individual counters. A newly deployed SD counter, and a schematic of the ground array read-out and communication module are shown in Figure 9.

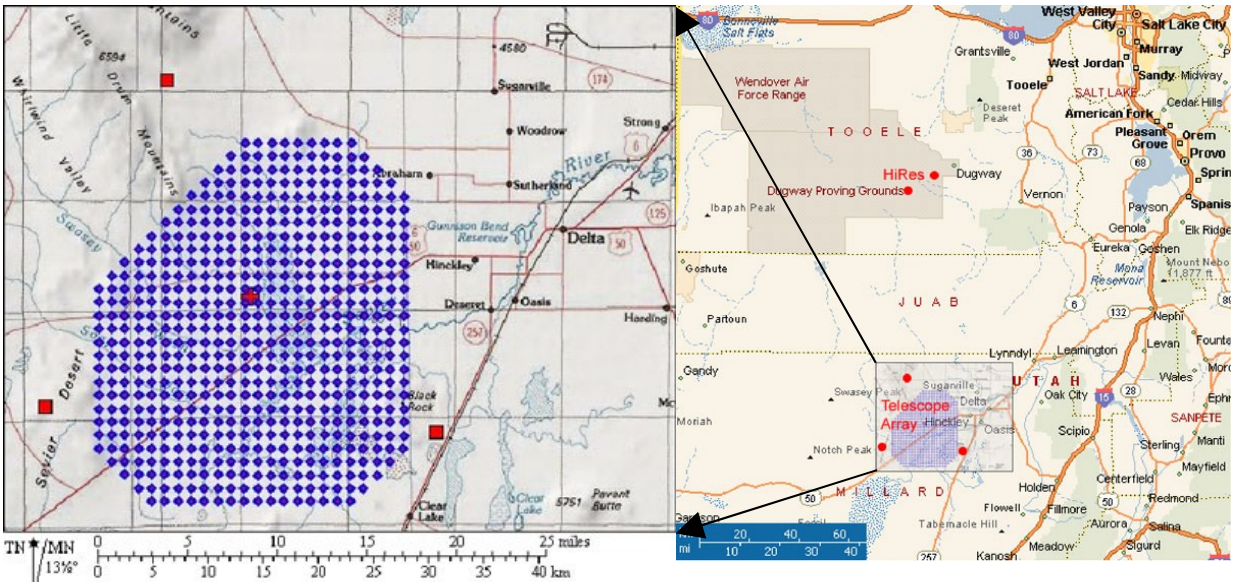

Figure 8: Map of the Telescope Array site showing the locations of the three exterior fluorescence stations (squares), the central laser facility (cross), and the positions of the scintillation counter (diamonds). The panel on the right shows the scale of the site in the context of a roadmap of north-central Utah. The two HiRes sites are indicated as circles about 80 miles north of the Telescope Array.

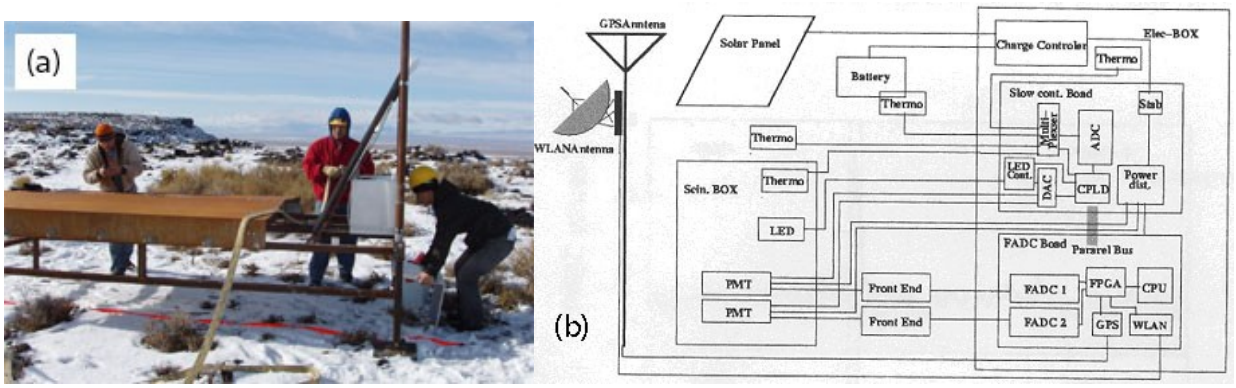

Figure 9: (a) A newly deployed SD scintillation counter. (b) Block Diagram of the read-out and communication module for the TA ground array station.

The TA-FD0 fluorescence Station at Black Rock Mesa is shown in Figure 10. The observatory building is equipped with three garage-style doors which open on clear, moonless nights to permit observations by the telescopes. A total of 12 telescopes are deployed in this building. The TA mirrors are 3.0 m in diameter, subdivided into 18 segments. These have an effective collection area that is about 30% larger than the HiRes mirrors (which are ~2.5m in diameter, but clover-shaped). As at HiRes, each telescope is instrumented with a 16×16 cluster of PMT pixels, arranged in a hexagonal grid. While these are larger PMTs (4") than those used by HiRes, each PMT views a 1.1° cone of the sky which is only a bit more than the HiRes telescopes. An identical building and set of telescopes are located at the TA-FD1 site at Long Ridge. The PMT cluster, mirror, and double-layered support structures are also shown in Figure 10.

The readout electronics for the TA-FD0 and TA-FD1 fluorescence detectors are very similar in concept to those of the HiRes systems. The design of this system was a collaborative effort between groups at Tokyo Institute of Technology, Osaka City University, and University of Utah. Each PMT channel is digitized by a 14-bit, 10MHz FADC system. This sampling rate is identical to that used by the HiRes-2 detector. The mirror trigger module (the so called Track-Finder, or TF board) uses a coincidence pattern search similar to that used at HiRes-1, and is designed by the same engineer, J. Smith (Utah). Mr. Smith also designed the site-wide Central Trigger (CT) module.

The TA-FD2 site at Middle Drum is instrumented with 14 reconditioned HiRes telescopes, each with a 2.5 m diameter, clover-shaped mirrors, and 16×16 clusters of 2" phototube cameras. The HiRes tubes have a 1.0° field of view, so that 14 are needed to provide the same azimuthal coverage as the other TA detectors. Apart from a new central-timing system (which provides GPS time stamps on individual mirror triggers) a rearranged inter-mirror trigger network, and a new Ethernet system, the TA-FD2 site is essentially identical to 2/3 of the old HiRes-1 detector component-wise. However, at Middle Drum the mirrors are arranged in two rings. The MD observatory views about 112° in azimuth and 3° to 31° in elevation. Middle Drum site is shown in an early installation phase in Figure 11.

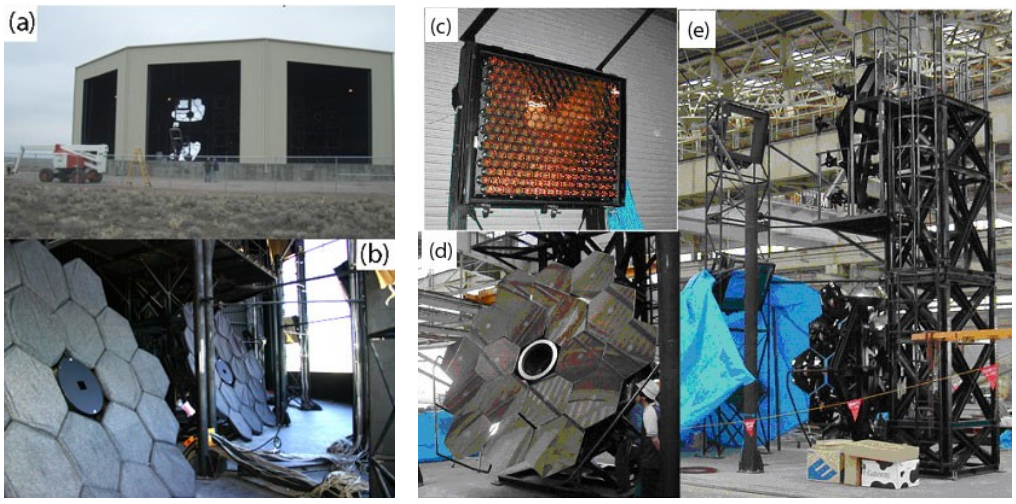

Figure 10: (a)TA-FD0 Fluorescence Building at Black Rock Mesa. (b) Interior shot of the BRM FD building showing covered mirrors. (c) A 16×16 4" PMT camera for the Telescope Array FD. (d) An 18-segment, 2.9 m diameter TA mirror. (e) A two-story mirror support structure showing one fully mounted mirror in the lower layer and empty brackets for the PMT clusters.

The surface array and the fluorescence stations are designed to make independent measurements of UHE cosmic rays. The ground array becomes fully efficient at above ~6×10^{18} eV. The FD stations each operate two *rings* of telescopes viewing 3° to 31° in elevation. Operating in monocular mode, each FD can measure cosmic ray showers down to ~3×10^{17} eV. Together, the three FD stations and the surface array operate in hybrid mode with an aperture that covers the entire array at energies above ~ 10^{19} eV. The FD stations can also observe showers in stereo mode, with limited aperture at 10^{19} eV that grows with increasing energy to cover the full ground array only at ~10^{20} eV.

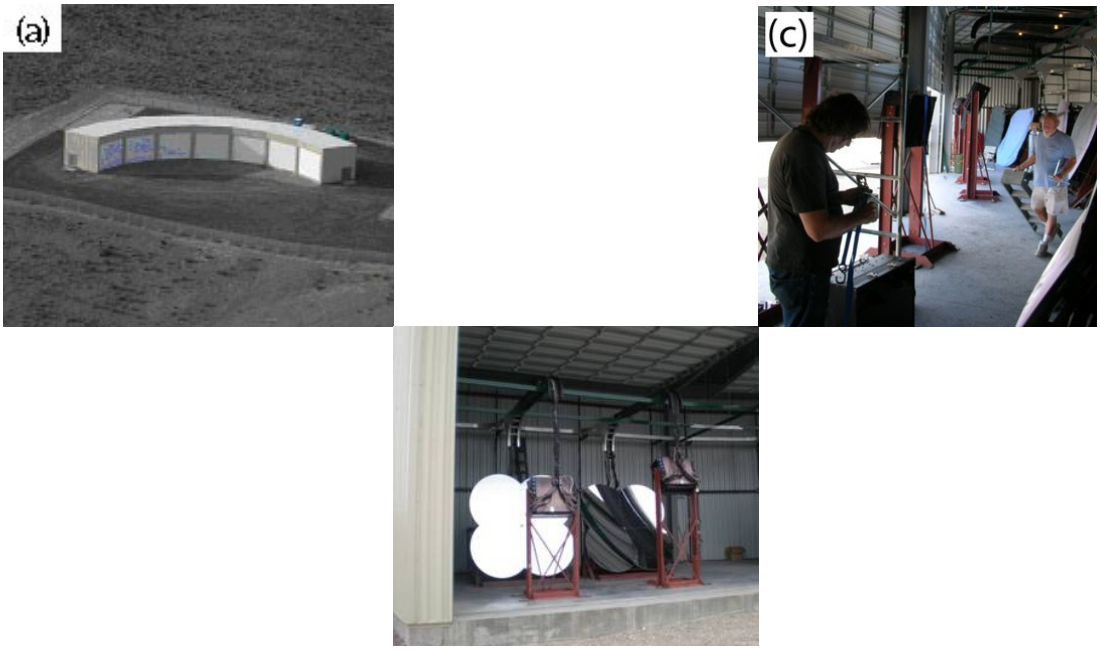

Figure 11: (a) Aerial view of the Middle Drum Facility. (b) Two installed and aligned telescopes at the MD site. Each bay contains two telescopes: a ring one telescope viewing 3°-17° in elevation and a ring two telescope viewing 17° to 31°. Each telescope has a 2.5 m diameter, clover-shaped HiRes mirror, (c) Telescope cameras being installed at Middle Drum. Each camera has 256 PMT pixels each subtending a 1.0° field of view.

The fluorescence and surface detectors of TA are all collecting data. The FD began observation in December, 2007, and the SD in May, 2008.

3.1 Analysis of Data from the TA Middle Drum Fluorescence Detector

The TA Middle Drum (MD) detector consists of reconditioned telescopes from the HiRes-I detector, and the data collected has been analyzed by the same programs used for HiRes-I. There is one very important difference: HiRes-I had one ring of telescopes that observed elevation angles of 3 to 17 degrees, where MD has two rings that cover elevation angles of 3 to 31 degrees. The longer tracks give additional information about the geometry and development profiles of cosmic ray showers. This results in two improvements of MD measurements over HiRes-I. First, events are reconstructed with better geometrical and energy resolution; and second, we can reconstruct lower energy events. Instead of the lowest energy being $10^{18.5}$ eV for HiRes-I, for MD it is $10^{18.0}$ eV.

In the HiRes experiment we introduced into the field an analysis method that emphasized simulating the exact conditions of the experiment using the Monte Carlo technique, and verifying the accuracy of the Monte Carlo simulation by making direct, detailed comparisons between the Monte Carlo results and the data. We proved that this method works very well for cosmic ray fluorescence detectors. It allowed us to calculate the aperture of the HiRes detectors very accurately. We have now applied that technique to the fluorescence detectors of TA. Again it works very well.

The method consists of generating a set of Monte Carlo (MC) events that should look exactly like the data, while using only inputs measured independently (we do not "tune" the MC). Development profiles of showers are taken from simulations, the spectrum and composition are taken from previous measurements, and showers are generated exactly as they would occur in nature. The generation of fluorescence light, its propagation to the detector, the optical elements, front-end electronics, and data acquisition system are all simulated. The result is written out in the same format as the data and analyzed with exactly the same programs. If the MC events are identical to the data in all distributions then one says, "We understand our detector", and one is assured that one can use the MC to calculate the aperture of the detector. "Comparison plots" of data and MC are crucial in this process. One example of the excellent MD comparisons, typical of many, is shown in Figure 12, a data – MC comparison of the impact parameter of events, shown in four energy bins.

Having confidence in our analysis and simulation, we now calculate the spectrum of cosmic rays. This is shown in Figure 13. Here the MD spectrum is compared with the HiRes monocular spectra. The two are in excellent agreement.

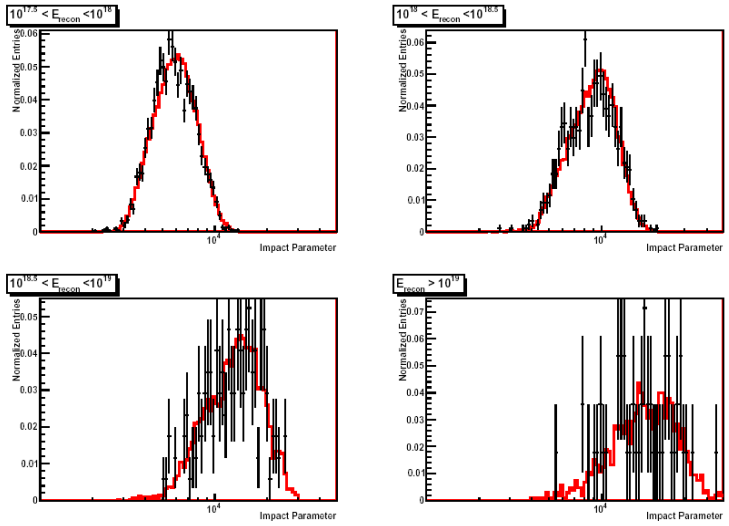

Figure 12. Data/Monte Carlo comparisons of the impact parameter of showers from the TA Middle Drum FD. Black points are data and MC is the red histogram. Results in four energy ranges are shown.

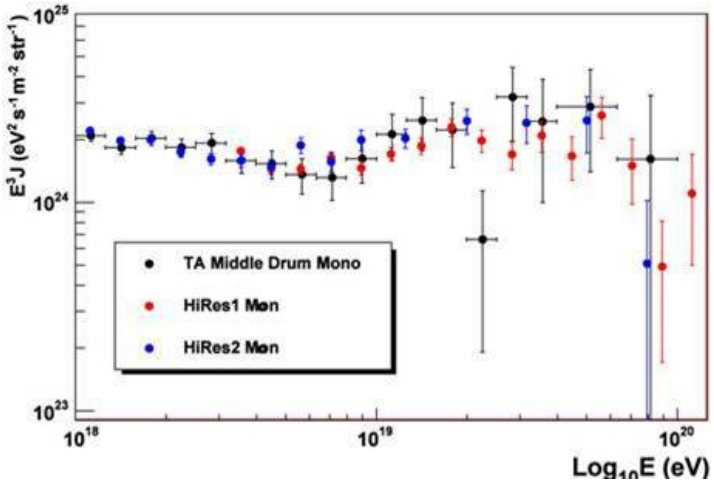

Figure 13. The cosmic ray spectrum measured by the Middle Drum FD compared with the HiRes monocular spectra. E^3 times the flux is shown. The two spectra are in excellent agreement.

3.2 TA Surface Detector Analysis

The first six months of TA SD data were collected independently by the three radio towers (and the sub-arrays of counters which they service). This configuration led to trigger inefficiencies near the center of the array. These data has been analyzed and the results are presented below. After November, 2008, the data of the SD array were collected as a whole without these trigger inefficiencies. As of October, 2009, these data are under analysis and events look identical to the earlier data.

We are carrying out a type of analysis which is new to surface detectors. We are applying the same data and Monte Carlo techniques described above, for fluorescence detectors in HiRes and TA, to the TA SD. To our knowledge this has never before been attempted.

The first step is generating a library of cosmic ray showers that accurately resemble data. We are using the shower Monte Carlo program Corsika [34] and hadronic generator QGSJetII [35], which are very widely used in the field. To avoid the enormous CPU requirements for simulating complete showers, an approximation called "thinning" is usually used. Here, once particles in the shower become lower in energy than some preselected fraction of the primary cosmic ray's energy, only a representative sample of particles is followed, but they are given weights to allow the total density of shower particles to be calculated. In the center of a shower where the number of particles is truly enormous the thinning approximation gives an accurate description of the shower process. This is the part of a shower that a fluorescence detector sees. However a surface detector works in the lateral tails of showers (counters near the center of a shower are almost always saturated and have limited usefulness) where the thinning approximation is quite inaccurate.

To solve this problem we invented a process, called "dethinning", to transform thinned showers into accurate representations of the shower process. First we developed a method of running Corsika in parallel on many CPU's, and generated about 100 showers, without thinning, of energies between 3 and 30 EeV. Then we used these showers as a standard of comparison in developing the dethinning process. Dethinning consists of replacing a thinned particle of weight w by w individual nearby particles. The trajectories are varied to reproduce both the mean and RMS of the particles' densities, and their arrival times at the ground. The results of dethinning are shown in Figure 14.

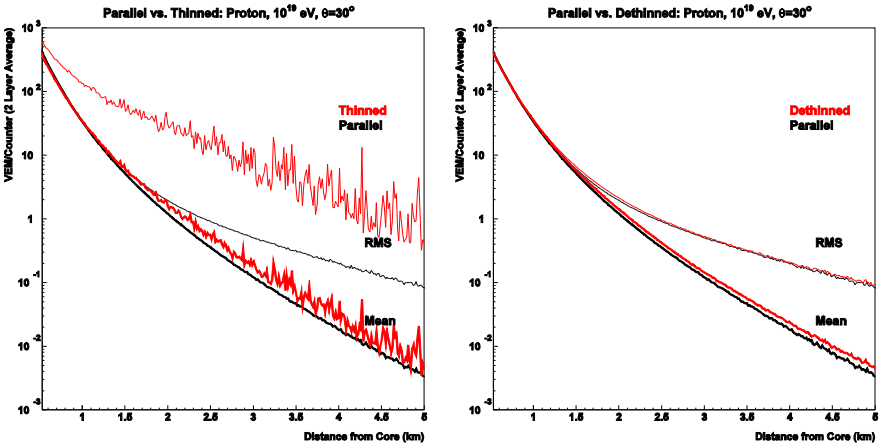

Figure 14. Results of "dethinning": the mean and RMS of Corsika showers as a function of distance from the core. The left panel shows in black the averages of 14 showers generated in parallel, and in red 14 almost identical showers thrown using the thinning approximation. The average particle densities are close but the RMS's are quite inaccurate. The right panel shows the result of our dethinning process. The same 14 thinned showers, having been dethinned, are shown in red.

We generated a library of dethinned showers indexed by energy and zenith angle. In the detector Monte Carlo program we place them on the SD array exactly as real showers would be

distributed. We then simulate the trigger, the front end electronics and data acquisition system, and write the simulated events in the same format as the data. We analyze both data and Monte Carlo events using exactly the same programs so we can make direct, detailed comparisons between the Monte Carlo simulation and the data. As in the FD case, excellent agreement between data and MC distributions in all cases would indicate a thorough and accurate understanding of the detector. We would then calculate the aperture of the detector as a function of energy, and measure the cosmic ray spectrum.

We have developed an SD analysis process for TA. It begins with a fit for the geometry of the shower using the "modified Linsley" function [36]. We tuned this function to the data by adjusting parameters until the residuals of the fit, in distance from the core, density of particles, and zenith angle, are centered at zero, and the residuals normalized to the fitting uncertainties are a bit less than unity. Figure 15 shows these normalized residuals as a function of particle density. When we fit the Monte Carlo events, generated so they follow the energy, composition, and geometry of real showers, we find that their fitting residuals are identical to the data. The Monte Carlo normalized residuals are also shown in Figure 15. Our fits to the lateral distribution function of showers (which is used to measure S800, the particle density at 800 m from the shower core) also has the same property of having identical residual distributions between data and Monte Carlo.

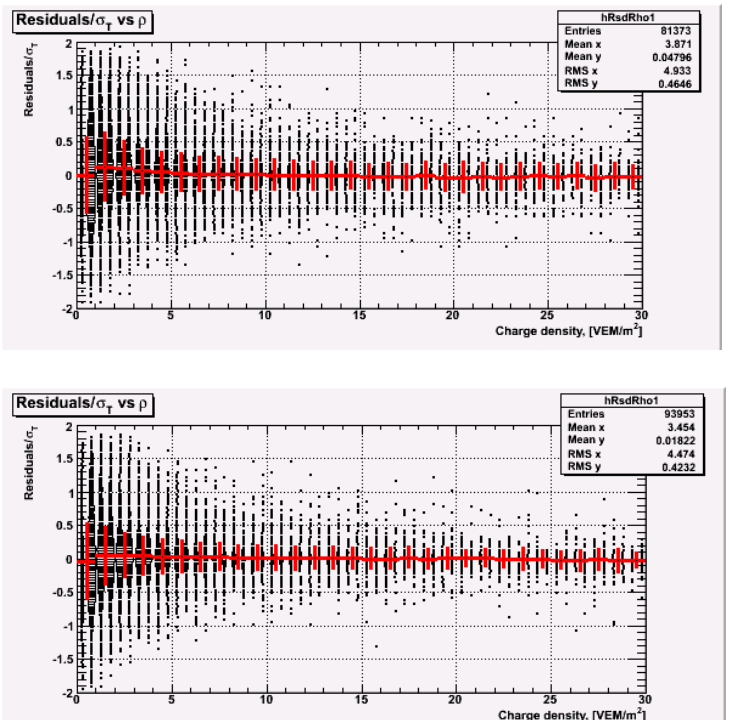

Figure 15. Residuals to the TA SD geometry fit in particle density, normalized to the fitting uncertainty. The data is the upper panel and the Monte Carlo is shown on the lower panel. They are essentially identical.

Since the same code is used to reconstruct both data and Monte Carlo events, we can ask whether the detailed comparisons between the two are identical or not; i.e., do we understand our detector well enough to use the Monte Carlo program to calculate its aperture. One comparison plot,

typical of many, is shown in Figure 16. This shows the number of SD detectors that are hit for events of energies above 4 EeV. The agreement is excellent, and is typical of all such comparisons.

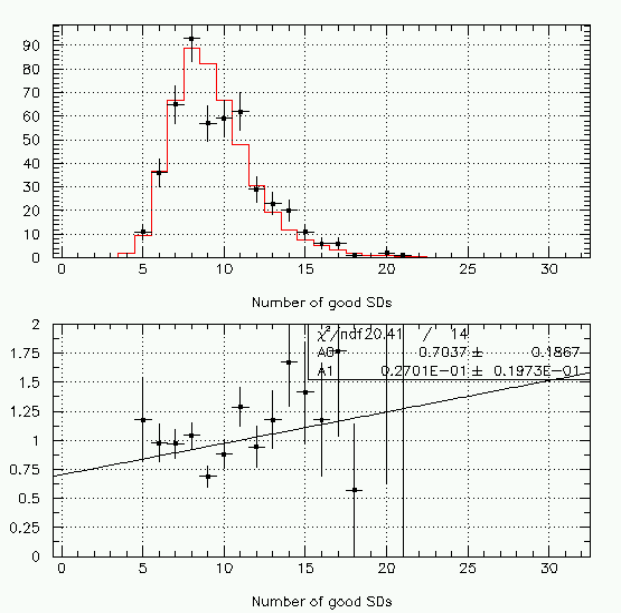

Figure 16. Comparison between the number of surface detector counters struck (for events of energy greater than 4 EeV) between data and Monte Carlo simulation. The data points are shown in black and the MC in red. The lower plot is the ratio of data/MC. The agreement between data and MC is excellent.

The determination of energies of SD events proceeds in two steps. First by interpolating the S800 and zenith angle values of data events with those of Monte Carlo events (where we know the generated energies) we make an energy estimate. By comparing these energy estimates for hybrid events with energies measured by the Middle Drum FD detector, we have measured a correction factor, which is 1.40±0.15, which we apply to the SD energies (the SD energies are lowered). This correction is necessary because of the fact that the energy scale of the Corsika and QGSJet programs has much larger uncertainties than measurements made by a fluorescence detector. A two-dimensional scatter plot of the energy estimates of hybrid SD events and the energies of the same events as measured by the Middle Drum fluorescence detector is shown in the upper panel of Figure 17.

The resulting spectrum is shown in the lower panel of Figure 17, along with the spectrum measured by the Middle Drum FD. They agree very well within statistics.

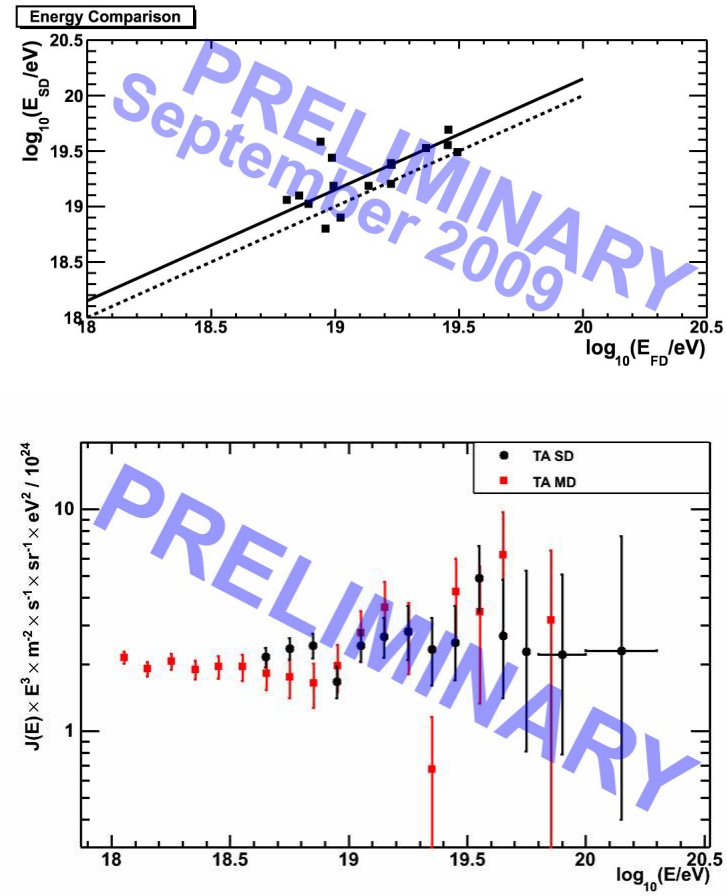

Figure 17. Upper panel: comparison of energies of hybrid events, measured by the TA surface detector and the TA Middle Drum fluorescence detector. SD energies are larger by a factor of about 1.4, and are normalized down by this factor to agree with the (more accurate) FD energy scale. Lower Panel: Telescope Array cosmic ray spectra measured using the TA Middle Drum (MD) FD data and the TA SD analysis reported here. These results are quite preliminary, and the statistics are as yet very limited, but the two spectra are in good agreement.

4 The TA Low Energy Extension Detectors

The TA Collaboration is currently preparing a new proposal to build a low-energy extension to the TA detector. The goal of the extension is to make multi-component observation of cosmic rays down to ~3×10^{16} eV. This will include (a) stereo fluorescence observations optimized for the ~3×10^{17}-10^{19} eV, a region that was not well covered by the stereo HiRes detector, (b) hybrid (fluorescence + scintillation counter) observations in the ~3×10^{16}-10^{18} eV energy region, which is well below the operating range of either HiRes or the main TA detectors, and (c) a muon detector system to provide an orthogonal composition measurement in the $10^{16.5}$-10^{18} eV range. We describe the instrumentation for each of these components in the following subsections.

4.1 The 6 km Stereo Detector

The fluorescence component of the TALE proposal will be placed at a new site designated TALE-FD, which is located near the TA-FD1 (Long Ridge) site. The location of the site, shown in Figure 18(a), is primarily determined by the availability of land under the aegis of the Utah

School and Institutional Trust Land Administration (SITLA) located within ~6 km of the Long Ridge FD (which also sits on SITLA land). The 6 km distance scale between TA/TALE FD pair is chosen to provide a maximum overlap between the TA and TALE FD apertures, while keeping enough detector separation to maintain good accuracy in geometrical reconstruction, comparable to that of the HiRes experiment.

The primary instrumentation at the TALE site will be provided by the 42 telescopes formerly deployed at HiRes-2. These telescopes have 2.5 m diameter, cover-leaf style mirrors identical to those deployed at the TA-FD2 (Middle Drum site), and phototube cameras that are similar. The 42 sets of HiRes-2 read-out electronics have software-adjustable front-end amplifiers (to equalize the overall individual channel gain over the entire detector) and 8-bit FADC digitizers running at 10 MHz. An additional 32 channels are also provided for the analog sums of rows and columns of phototubes to reconstruct the signal in the event of overflows in individual channels. In comparison, the new TA FD electronics use 10-bit 40 MHz FADCs, however they perform a digital sum over four time-bins to provide an effective 12-bit dynamic range at 10 MHz. The smaller dynamic range of the TALE/HiRes electronics is not expected to be a problem for the stereo observation, which will focus on the 10^{18}-10^{19} eV energy decade in order to improve stereo measurement through the "ankle" region over that of HiRes.

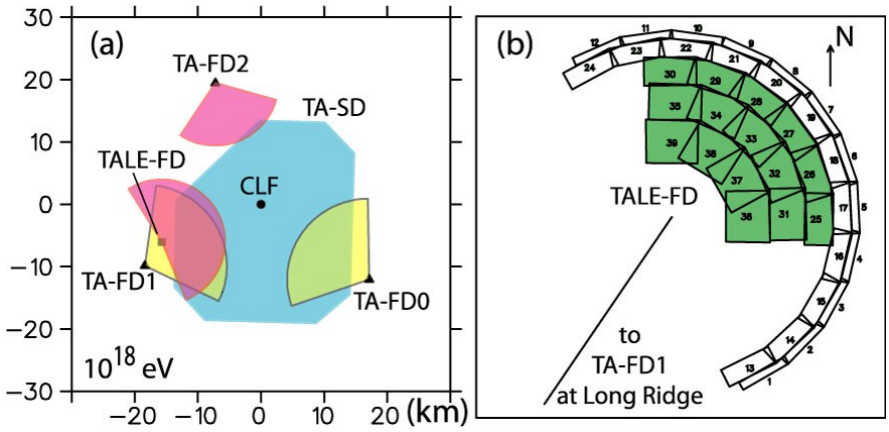

Figure 18: (a) Layout of the TA/TALE surface array and Fluorescence Detector Sites. The shaded yellow and pink wedges show the approximate fluorescence coverage at 10^{18} eV. (b) The sky coverage (projected onto the horizontal) of the telescopes at the TALE site near the TA-FD1 site at Long Ridge. In this view, the telescopes of the TALE Tower detector are shaded in green.

The first 24 of these telescopes will be redeployed in the same two-ring arrangement as TA-FD2 (Middle Drum site) that covers elevation angles from 3° to 31°. This is what we call the 6 km Stereo Detector or 6 km TALE. The azimuthal distribution of these telescopes, shown in Figure 18(b), was chosen (by simulation studies) to maximize the stereo aperture at 10^{18} eV, within the constraint of the available location. The shaded wedges in Figure 18(a) gives an illustration of the overlap between the viewing range (calculated for vertical showers) of the TALE-FD telescopes and that of the TA-FD1 station at 10^{18} eV. At this energy, the range of the telescopes at the TA sites are slightly longer than HiRes telescopes due to their ~30% larger mirror collection areas.

With the TALE-FD site arranged as shown in Figure 18, the TALE stereo aperture is relatively flat in comparison with the HiRes stereo aperture (see Figure 19). The 6 km TALE aperture changes by less than a factor of 10 from 10^{19} eV to 10^{18} eV, whereas the HiRes stereo aperture

drops by more than two orders of magnitude over the same decade. In particular, the TALE stereo aperture is more than five times that of HiRes at 10^{18} eV. The improvement in the aperture comes from a combination of two factors: (a) In each of the two TALE pairs, both detector stations will have two rings of mirrors, covering up to 31° in elevation, whereas the HiRes-1 site only had one ring of mirrors, covering up to only 17°; and (b) The factor of two reduction in the TALE site spacing from that of HiRes (12.5 km) significantly improves the overlap between the detector pairs towards the low end of 10^{18}-10^{19} eV energy decade.

Simulation studies have confirmed that the detector resolutions of the stereo TALE pairs are comparable to that of the HiRes detector (~15% energy, ~0.6° angle, and ~30 g/cm^2 X_{MAX}) in the target 10^{18}-10^{19} eV range (see Figure 19(b) and (c)). Moreover, because of the better overlap, the aperture calculation will be less sensitive to energy scale determination, atmospheric characterization and other systematic uncertainties. In the HiRes measurement, most of the systematic uncertainties in the aperture were contained at the cost of energy-dependent restrictions on acceptance, which further limited the stereo aperture towards the low end. The TALE 6 km stereo data will retain HiRes' advantage of having redundant measurements, which is crucial for the validation of the detector resolutions determined from the Monte Carlo simulations in the relevant energy range. This is one distinct advantage of the stereo method over that of simple hybrid. In particular, with stereo, one can study composition using the full X_{MAX} distribution in a given energy bin, without blindly relying on simulation results or on extrapolating stereo results from a different energy range (as is in the case of AUGER).

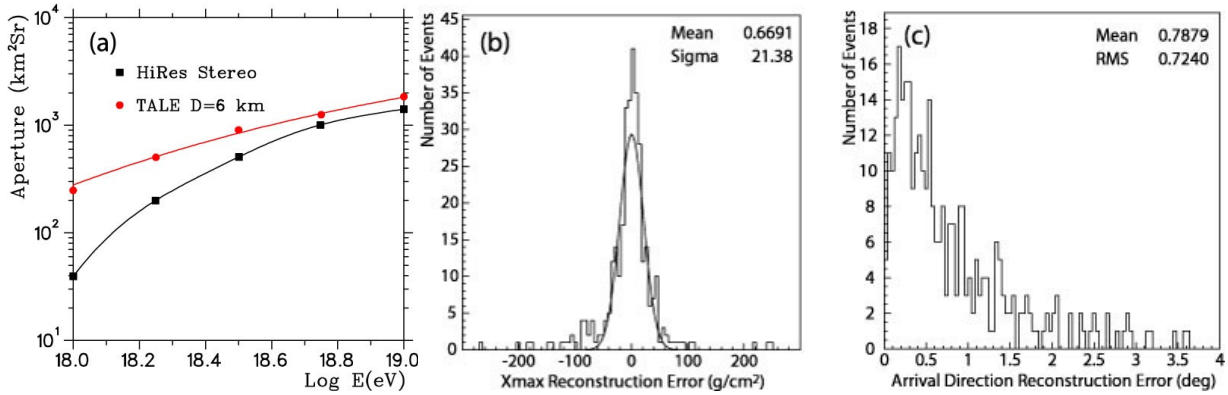

Figure 19: (a) A comparison of the (instantaneous) stereo aperture of the TA/TALE FD pairs (upper curve, red) and the HiRes stereo (lower curve, black) (b) X_{MAX} resolution, and (c) angular resolution of the TA/TALE stereo pair detectors from simulation studies.

In addition to providing improved (over HiRes) stereoscopic measurements through the ankle region, the 6 km TALE fluorescence detectors will also provide stereo coverage over half the ground array at 10^{19} eV, and over the full SD above ~3×10^{19} eV. This rather serendipitous feature is illustrated in by the overlap diagram in Figure 20(a). The expected improvement of the angular resolution (to ~0.1°) over that of hybrid or stereo alone will significantly enhance TA's ability to study small-scale anisotropy. Furthermore, Figure 20(b) illustrates the combined monocular aperture of the TA and TALE fluorescence detector. Assuming 10% duty cycle (from the HiRes and Fly's Eye experience for the western Utah Desert), the total time-averaged aperture of TA will approach 2,200 km^{2}sr (~1/3 of the Southern AUGER surface array).

4.2 The Tower Hybrid Detector

With the two-ring configuration of mirrors, the effective physics threshold of the TA/TALE pairs will be ~10^{18} eV. In order to study the "second knee" structure that occurs in the 10^{17}-10^{18} eV decade, we will need to build a fluorescence detector with a field of view that extends well above 31°. A previous attempt at studying this region was made by the joint observations between the HiRes prototype detector and the MIA muon array at Dugway, Utah. The HiRes-MIA hybrid experiment operated from 1993 through 1996. The first 14 telescopes at the HiRes-1 site were arranged in a tower configuration: two telescopes each at 3°-17° (ring 1) and 17°-31° (ring 2), three telescopes each at 31°-45° (ring 3) and 45°-59° (ring 4), and four telescopes at 59°-73° (ring 5) in elevation coverage. The HiRes Prototype tower was operated both in monocular mode and in hybrid mode with the MIA array (with the CASA array providing the surface trigger, but using the MIA timing to constrain the geometrical fit). This combination of detectors was far from optimal, because CASA and MIA were designed to search for gamma ray induced air showers in the 10^{14}-10^{16} eV range, whereas HiRes telescopes were optimized for observations above 10^{18} eV. The result is an overlap of the lowest reaches of the HiRes prototype detector statistically limited by the 500m×500m size of the CASA-MIA arrays. Moreover, the MIA array was designed as a cosmic ray veto muon detector. The 1024 individual scintillators each provided only one bit (hit/no-hit) of information, and could not actually count the number of muons. The HiRes Prototype tower and CASA-MIA were separated by about 3.5 km.

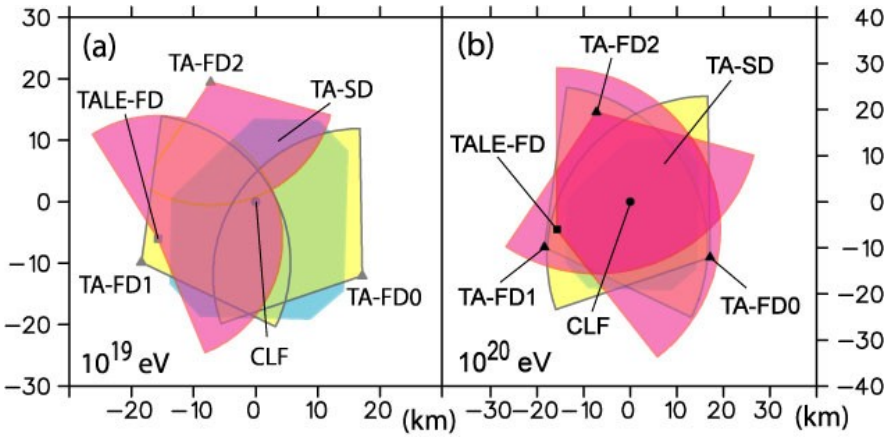

Figure 20: The fluorescence apertures of the TA and TALE fluorescence stations at (a) 10^{19} eV, and (b) 10^{20} eV. At above 10^{19} eV, the stereo coverage extends over the western half of the ground array. At 10^{20} eV, the combined monocular (time-averaged) fluorescence, and ground array apertures will approach 2,200 km^{2}sr.

As a part of TALE, we propose to build a new tower detector at the TALE-FD station. This part of TALE will also include an infill ground array for hybrid coverage, and a muon array to provide an orthogonal composition measurement. Above the ring-1 and 2 telescopes that the tower will share with the 6km stereo detector, the tower will consist of 6, 5, and 4 telescopes each in rings 3, 4 and 5, respectively. The sky coverage of the 15 tower telescopes are shown by the green shaded boxes in Figure 18(b). The choice for the TALE-FD site to be near Long Ridge instead of Black Rock MESA, and the geometrical arrangement of the Tower telescopes are both determined by the availability of suitable land for the infill array and muon detectors northeast of the TALE-2 site within the boundaries of the TA main ground array. A preliminary baseline design for a Ring-4 Tower telescope is shown in Figure 21.

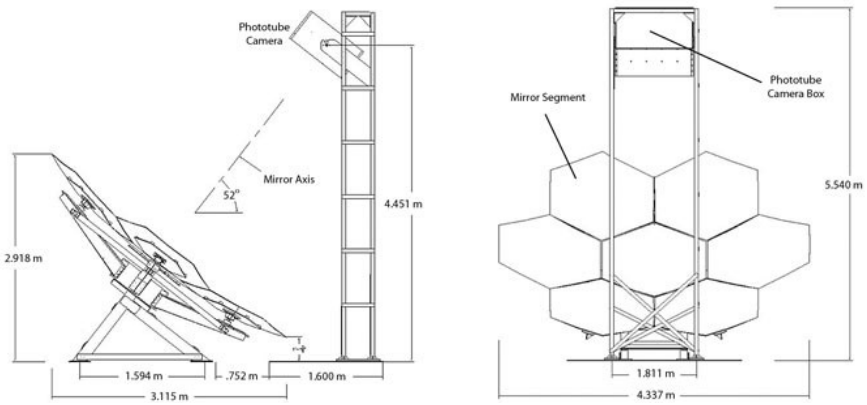

Figure 21: Two orthogonal views of a Ring-4 TALE tower telescope. The segmented mirror has an effective collection area ~3 times that of the HiRes-style mirrors used for the two lowest rings of the TALE telescopes.

The TALE tower detector represents a significant improvement over the HiRes prototype in three ways: (1) the increased number of telescopes (from 14 to 25 effectively) reduces the edge effect which was a major limiting factor in the HiRes-MIA measurements; (2) the infill scintillation array and the muon array will be optimized to work in the same $10^{16.5}$-$10^{18.0}$ eV energy range as the fluorescence detector, and (3) the three upper rings (3-5) of the TALE tower telescopes will use 4.4 m diameter mirrors which have ~3 times the collection area of the HiRes mirrors, substantially improving the sensitivity at the lowest energies. The histograms in Figure 22(a) show the expected number of events collected over a six-month observation period for three scenarios. As seen in the plot, the increased size of the tower mirrors will yield an order-of-magnitude increase in the event sample in the relevant $10^{16.5}$-$10^{18.0}$ eV energy range.

In addition to improved sensitivity, the high elevation coverage of the tower mirror will also remove the acceptance bias towards deeper X_{MAX} events that limited HiRes stereo composition measurements to above 10^{18} eV. This effect is shown in Figure 22(b). This acceptance bias results from the limited elevation (<~31°) of the 2-ring design of HiRes (which was adopted by AUGER). The 5-ring configuration of the Tower detector will eliminate this effect and allow TA/TALE to make an unbiased composition measurement down to 3×10^{16} eV.

4.2.1 Tower Detector Prototype Tests

We have constructed a prototype of the tower detector shown in Figure 21 atop Five Mile Hill at the U.S. Army Dugway Proving Ground, where the HiRes-1 detector was located. This detector used existing mirror segments from a previous experiment, which we configured to yield twice the area of HiRes mirrors (instead of the proposed 3× for tower detectors for TALE). The resulting telescope was pointed to ring 4.

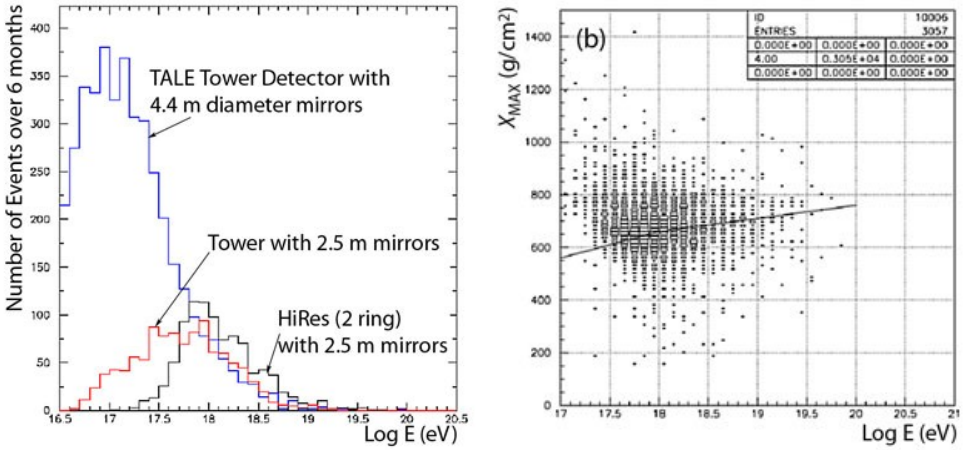

Figure 22: (a) A comparison of the number of expected events, for a 6-month running period, per energy bin (0.1 in $\log_{10}$ energy), for the TALE Tower detector with 4.4 m diameter mirrors (blue), TALE tower detector with 2.5 m diameter HiRes mirrors (red) and a standard HiRes/TALE 2-ring detector with 2.5 m diameter HiRes mirrors. (b) A comparison of the average Xmax (solid line) measured by the HiRes and HiRes-MIA experiments and the distribution of X_{MAX} of HiRes events (2-d histogram), demonstrating the trigger bias inherent in a 2-ring fluorescence detectors like those used by HiRes and AUGER.

We collected data with this detector, plus five HiRes1 telescopes pointing to ring 1, in July and August, 2007. The purpose of the test was to study the sky brightness, trigger rates, and light collection of the prototype mirror. The sky brightness and trigger rates were well within the ability of our electronics to handle. For example, the ring 1 mirrors triggered at about 0.5 Hz each, and the tower mirror triggered between 1 and 2 Hz. We observed cosmic ray events in the ring 1 mirrors, in the ring 4 mirror, and some in both rings' mirrors. Figure 23 shows one of the latter events. The top left panel shows the hit tubes in azimuth and elevation, and the top right panel shows the trigger time of phototubes vs. the angle of the tube in the plane that contains the shower and detector. From the time vs. angle plot we can reconstruct the geometry of the event: the perpendicular distance from the detector to this shower was 3.82 ± 0.04 km.

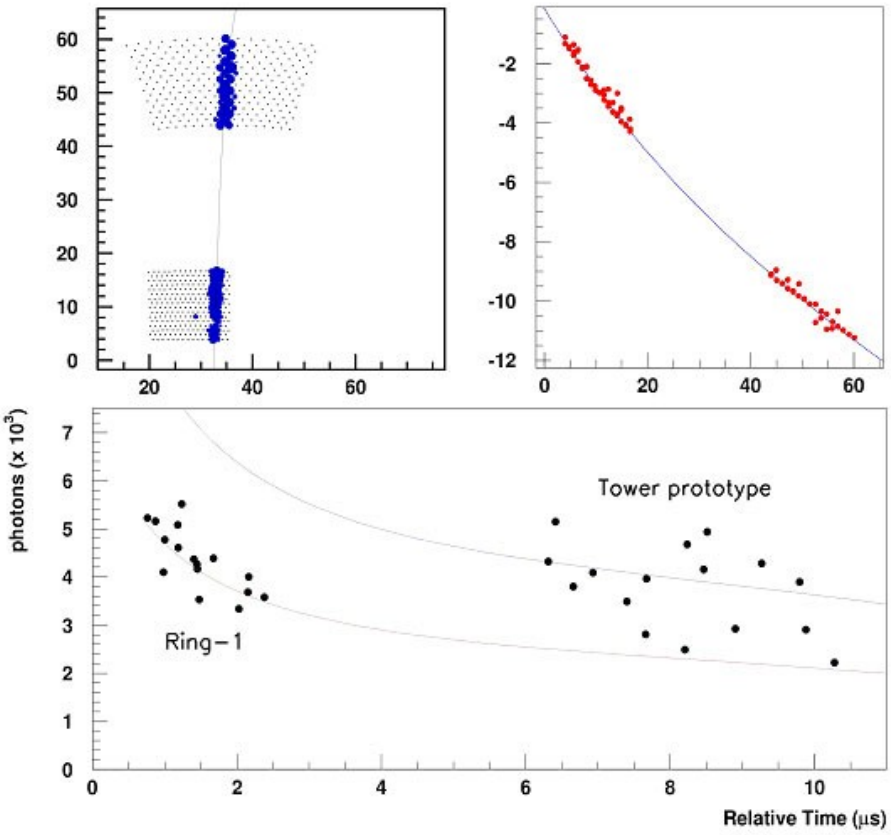

Figure 23 Tower prototype detector tests. The upper left panel shows a cosmic ray event seen in both the ring 1 (HiRes size) and ring 4 (Tower prototype) mirrors, in azimuth vs. elevation angles. The upper right panel shows the tube trigger time vs. angle in the shower-detector plane. Curvature in this plot allows us to determine the geometry of events, and this event is very well-determined. The lower panel shows the light collected from a Xenon flasher event 3.4 km away from the detectors. The expectation for the HiRes-size ring 1 mirror and for the (double-size) tower prototype mirror are both shown.

We also collected data while firing a Xenon flasher 3.4 km from the detector. The advantage of analyzing flasher events, in addition to having pre-determined geometry, is that the light collected at each phototube can be predicted from the known light-scattering properties of the atmosphere. The bottom panel of Figure 23 shows the number of photons collected as a function of arrival time at the phototube. We predicted the ratio of light collected in the tower prototype mirror to the HiRes mirror in ring 1 to be 0.94, and measured 0.86 ± 0.18, in excellent agreement with the prediction. The prototype detector performed to our expectations.

4.3 The Surface Infill Array

In order to extract the best geometrical reconstruction from the tower FD, TALE will also deploy an infill array of 100 scintillation counters identical to those of the main TA ground array. The new counters will be arranged in a square grid with a 400 m nearest-neighbor separation (see Figure 24). The SD array counters of the main TA array will also serve as part of the infill array, at the locations where the two coincide. In the arrangement shown, the surface infill array will allow hybrid reconstruction of events to ~3×10^{16} eV. These counters will also extend the SD energy reach of TA to below ~3×10^{17} eV. Funding for the infill array is being requested from the

Japanese government and the construction is planed to be a joint venture between the University of Tokyo, ICRR and Osaka City University.

4.4 Muon Detectors

To compliment composition measurements by the X_{max} technique, TALE will also measure muon content of the air showers. The greatest sensitivity of muon richness to primary particle composition is obtained by measuring the ratio of muon density to electron density (μ/e ratio) at the Earth's surface and at a fixed distance from the shower core (core distance). Previous experiments, such as Akeno and HiRes-prototype/MIA, used a core distance of 600m. However, our preliminary simulation results show that a more robust result is obtained at 300m, a distance we should be able to bracket over most of the TALE energy regime. Figure 25 shows the simulation results at a core distance of 300 m. In the plot we see the muon to electron density ratio, at 300 meters from the shower core, for three years worth of simulated TALE data. This simulated data incorporates a composition model which is 50% protons at 10^{17} eV which increases to 80% protons at $10^{17.9}$ eV. The fit to the simulated data is shown with the curves for pure iron and proton EPOS simulations.

Here we see predicted μ/e ratios, represented by the solid curves in Figure 25(b), which is 30%-50% greater for iron primaries, in comparison with proton primaries, within the energy range of interest to TALE.

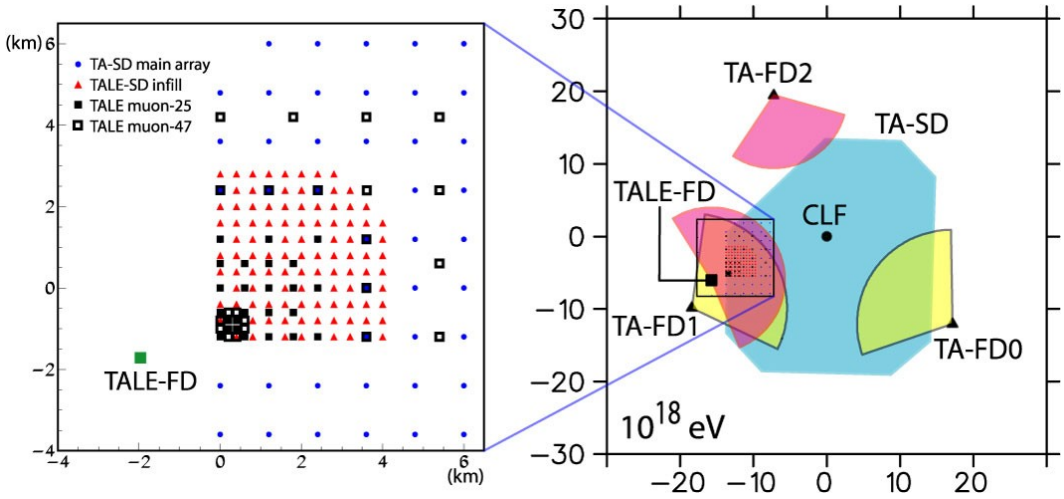

Figure 24: The TALE infill array, on the left, showing the layout of the various detector elements. On the right we see the location of the infill array with respect to the main TA detectors including the field-of-view of the TA-FDs and the tower detectors.

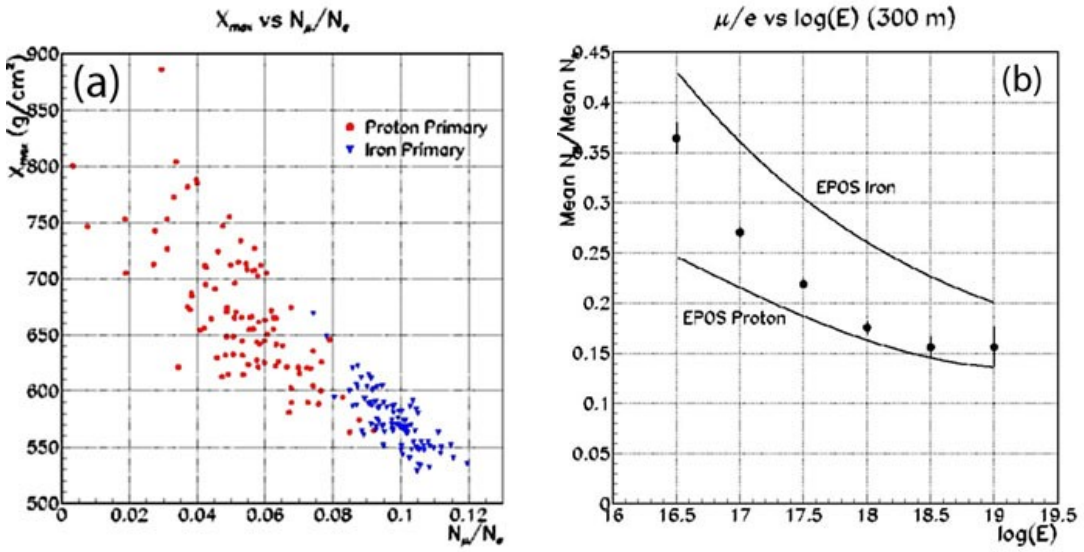

Figure 25: (a) Mean depth of shower maximum, X_{max}, versus muon to electron ratio, N_μ/N_e, 100 m from the shower core, for 10^{17} eV CORSIKA showers at 30 degree zenith angle. 100 proton (red circles) and 100 iron (blue triangles) induced showers are shown, illustrating complementary p-Fe separation using the two methods. (b) Simulated 3-year TALE signal for muon to electron density ratio at 300 meters from the shower core, at zenith angles of 25-35 degrees, for a composition change in the 10^{17}-10^{18} eV decade. This simulated data incorporates a composition model which is 50% protons at 10^{17} eV which increases to 80% protons at $10^{17.9}$ eV. The fit to the simulated data is shown with the curves for pure iron and proton EPOS simulations.

To discriminate between proton and iron primaries, each TALE muon detector station will consist of 12m^2 of scintillators placed under 10 ft. of earth overburden, in order to absorb the electro-magnetic part of the shower. This will give the detectors a muon threshold energy of about 0.8 GeV. Under the filter, the detectors will be essentially identical to the surface scintillator detectors. They will consist of one-cm thick scintillators coupled to PMTs by wavelength-shifting fiber, an arrangement which has been shown to give uniformity of response to muons of better than 7% in the standard TA surface detectors. The PMTs will be read out using a FADC and the signals relayed by a wireless network to the same central control for triggering and data storage.

For the earth overburden, we are investigating two possible designs:

1. Buried (underground) scintillators: This is the mechanically simplest and likely the least expensive option. A schematic of a buried muon detector is shown in Figure 26. We are currently exploring various approaches toward obtaining BLM permission to excavate and bury counters. One potentially promising idea is to integrate the muon detector construction with a project to evaluate the effectiveness of mine reclamation procedures on disturbed land areas.
2. Surface overburden: In this scenario the scintillator is placed at ground level, and earth is placed on top of it, either in an exposed berm, or within an enclosure (e.g. a steel shipping container), as illustrated in Figure 27. While more expensive, this option may be more acceptable to the BLM and would also be portable, should subsequent physics results suggest that a re-arrangement of the array would be advantageous.

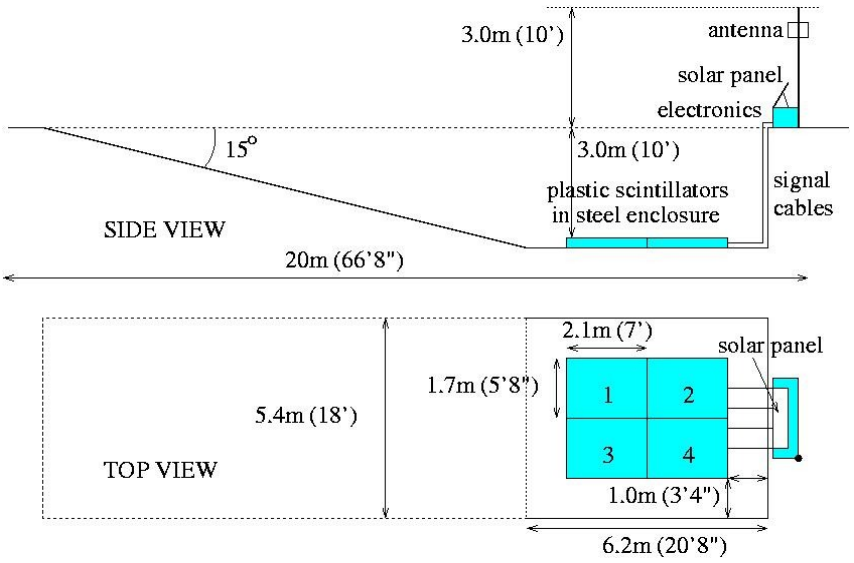

Figure 26: Schematic layout of a muon detector consisting of four scintillator modules buried at a depth of 10 feet (3 m). Each scintillator module (1.5m×2m = 5'×6'8") is contained in a 1.7m×2.1m (5'8"×7') stainless steel protective enclosure. A ramp of ~15° gradient is likely to be needed to lower the scintillators into the pit. At the far end of the pit, a solar panel will be mounted on a steel frame that also contains an electronics enclosure. A 3m (10') tall antenna is required for data transmission.

Figure 24 shows the layout of an array of 47 muon detectors within the field of view of the TALE tower detector. The array spacing is graded such that the density of counters decreases away from the TALE-2 site. This arrangement will provide hybrid reconstruction of events, along with simultaneous X_{max}, muon, and electron density measurements between $10^{16.5}$ eV to 10^{19} eV. At any given energy, the typical "best measure" of muon density will be ~1/ m^2. Our current plan is to construct only eight of the central 16 counters (a square of four in the middle with four more diagonally projecting out from the corners), and to exclude those counters located at more than 3 km from the inner (southwestern) corner of the infill array. This makes for a total of 25 muon counters. This configuration gives us muon coverage up to $10^{18.5}$ eV. At and above that energy the HiRes experiment had already the composition to be basically protonic.

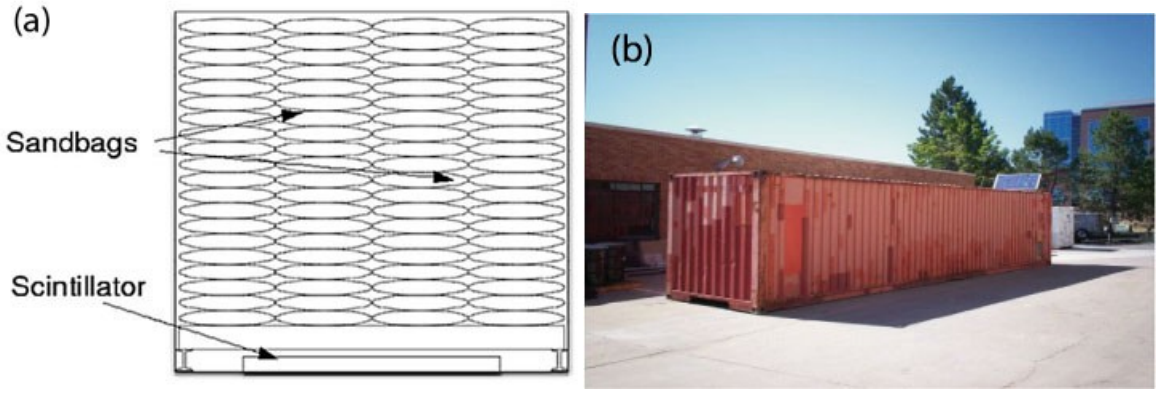

Figure 27: (a) Schematic cross-section of muon detector prototype contained in a steel shipping container (conex box). Approximately two meters of sand sit on top of the steel false floor, while the scintillator detectors slide underneath the sand filter. (b) A muon detector prototype under construction at University of Utah. A solar panel (on the roof at the far end of the conex box) provides power for the PMTs, readout electronics, and wireless LAN communications.

The data points in Figure 25(b) show the estimated 3-year TALE signal in a μ/e ratio measurement for a full complement of 47 detectors. For the 25 detector version we are planning we would simply lose statistical power above $10^{18.5}$ eV. The study assumed a composition transition in the 10^{17}-10^{18} eV decade. These points were obtained from a Monte Carlo simulation using muon distributions taken from CORSIKA showers, and with detector resolutions simulated. Removing the outer most detectors beyond 3 km, we lose sufficient statistics to make a useful measurement at energies above 10^{18} eV. Removing eight out of the 16 inner most counters reduces our sampling power for the lowest energy point, for which the error bar would grow by a factor of $\sim\sqrt{2}$. With 25 or more counters, the TALE muon detector composition measurements will provide an excellent complement to the X_{max} technique for studying composition in the second knee region. A prototype muon station, shown in the photograph of Figure 27(b), is currently under construction at the University of Utah, and will be site-tested in early 2008.

5. Physics Priorities

Since the TALE experiment consists of a number of detectors specialized to perform several physics measurements, it is relevant to express our opinions about what the TALE physics priorities should be. Since the whole focus of the experiment is understanding the physics of cosmic rays at energies lower than can be accessed by the TA, HiRes, or Auger experiments, the highest priority must be the measurements of the spectrum and composition in the energy range $16.5 < \log(E) < 18.0$. This energy range directly accesses the galactic/extragalactic transition and the energy and nature of the second knee of the cosmic ray spectrum. Answering the composition question in this energy range will also address the profound difference between the published HiRes and preliminary Auger composition results. Although these results have been measured at higher energies, the physical interpretation of composition measurements is dependent on the whole picture, from below the transition to the highest energies.

One important aspect of the TALE measurements is the fact that the energy scale will be known from first principles. The high energy part of TA/TALE will observe the GZK cutoff, which is known to occur at 5-6 x 10^{19} eV. The high energy part of the experiment is operating now. Many events will be seen in coincidence between the fluorescence and surface detectors of TA, and the fluorescence and infill detectors of TALE, so cross calibration of energy scales will be straightforward.

For the TALE design described in this document, with an independent TALE fluorescence site, once we make the composition and spectrum measurements at the lowest energies, the physics of the ankle of the cosmic ray spectrum will come automatically. This is because the TALE fluorescence site will inherently have a good stereo aperture with a TA fluorescence detector. However, if the TALE fluorescence detectors were to be located at one of the TA fluorescence sites then the stereo aperture would be lost.

Finally, there comes the question of the second method of measuring composition; i.e., using the μ/e ratio. This method holds considerable promise, particularly in the context of an experiment where fluorescence and hybrid information is available. Historically the Kascade experiment

collected electron-positron and muon information for cosmic ray showers of energies from just below the knee to about 10^{17} eV. Their finding evidence for a rigidity-dependent composition change at energies above the knee was a significant accomplishment. Their density of detectors was higher than what we are proposing. Since one expects to see a simpler composition change above $10^{16.5}$ eV (the iron knee should be about 8×10^{16} eV, so in TALE we expect to see a heavy-to-light composition change above this energy), denser detectors are not needed. The addition of fluorescence detectors, with their absolutely known energy scale, and their operation in hybrid mode with the electron-positron and muon detectors, will be an important addition in the TALE case. We know that the <Xmax> method will be sufficient for TALE composition measurements, and we expect that by using the μ/e ratio method we will observe the galactic/extragalactic transition independently.

References